

# Hydrologic Characterization of Desert Soils with Varying Degrees of Pedogenesis:

## 2. Inverse Modeling for Effective Properties

Benjamin B. Mirus, Kim S. Perkins, John R. Nimmo,\* and Kamini Singha

To understand their relation to pedogenic development, soil hydraulic properties in the Mojave Desert were investigated for three deposit types: (i) recently deposited sediments in an active wash, (ii) a soil of early Holocene age, and (iii) a highly developed soil of late Pleistocene age. Effective parameter values were estimated for a simplified model based on Richards' equation using a flow simulator (VS2D), an inverse algorithm (UCODE\_2005), and matric pressure and water content data from three ponded infiltration experiments. The inverse problem framework was designed to account for the effects of subsurface lateral spreading of infiltrated water. Although none of the inverse problems converged on a unique, best-fit parameter set, a minimum standard error of regression was reached for each deposit type. Parameter sets from the numerous inversions that reached the minimum error were used to develop probability distributions for each parameter and deposit type. Electrical resistance imaging obtained for two of the three infiltration experiments was used to independently test flow model performance. Simulations for the active wash and Holocene soil successfully depicted the lateral and vertical fluxes. Simulations of the more pedogenically developed Pleistocene soil did not adequately replicate the observed flow processes, which would require a more complex conceptual model to include smaller scale heterogeneities. The inverse-modeling results, however, indicate that with increasing age, the steep slope of the soil water retention curve shifts toward more negative matric pressures. Assigning effective soil hydraulic properties based on soil age provides a promising framework for future development of regional-scale models of soil moisture dynamics in arid environments for land-management applications.

ABBREVIATIONS: ERI, electrical resistance imaging; SER, standard error of regression; TDR, time domain reflectometry.

AS PART OF a broader study to better understand the ecologically sensitive habitat of the Mojave Desert, a series of field experiments in the Mojave National Preserve has examined undisturbed alluvial deposits of differing ages and their associated soil hydraulic properties (Nimmo et al., 2009). Extensive geologic mapping for the region (Miller et al., 2009), along with a set of transfer functions relating deposit age to soil hydraulic properties, is expected to facilitate future development of a regional-scale model, based on Richards' equation, of unsaturated-zone dynamics within the near surface. Such a model requires that soil water retention curves and unsaturated hydraulic conductivities be assigned for each hydrogeologic unit. Using the available data, a framework was needed to determine the appropriate parameter values and assign their spatial distribution based on soil age.

The objective of the work presented here was to use inverse modeling techniques to estimate effective parameter values of soil hydraulic properties for three alluvial deposits of contrasting age

examined by Nimmo et al. (2009). The variably saturated flow model VS2D (Lappala et al., 1987; Hsieh et al., 2000) was used in conjunction with the universal inverse code UCODE\_2005 (Poeter et al., 2005) to explicitly account for the effects of soil layering and antecedent moisture on lateral spreading during ponded infiltration. A secondary objective of the inverse modeling was to improve understanding of how soil age influences soil hydraulic properties in the Mojave Desert in the context of plans to develop a regional-scale model of soil moisture dynamics. Related to this long-term goal of the Mojave work, the primary question addressed here is whether the restrictive assumptions and simplifications necessary for a regional-scale model still allow an approach based on Richards' equation to mimic the ecologically important unsaturated flow observed in the field for different soil ages with varied degrees of pedogenic development.

The fundamentals of soil–plant–water relations intrinsically emphasize meter and submeter scales, whereas modeling for land use management purposes requires attention to kilometer scales and greater. This study focused on bridging these disparate scales through a possible correlation of effective soil hydraulic properties with soil developmental classifications that can be mapped at an intermediate scale.

### Measuring Soil Hydraulic Properties

Although laboratory measurements using core samples are potentially the most accurate determinations of water-retention curves and unsaturated conductivity, these methods present certain problems, including: (i) disparity between scales of measurement and modeling, (ii) difficulty in sampling unconsolidated sediments

B.B. Mirus, K.S. Perkins, and J.R. Nimmo, U.S. Geological Survey, 345 Middlefield Rd., MS 421, Menlo Park, CA 94025; K. Singha, Geosciences Dep., 503 Deike Bldg., Pennsylvania State Univ., University Park, PA 16802. Received 3 Mar. 2008. \*Corresponding author (jrnimmo@usgs.gov).

Vadose Zone J. 8:496–509  
doi:10.2136/vzj2008.0051

© Soil Science Society of America

677 S. Segoe Rd. Madison, WI 53711 USA.

All rights reserved. No part of this periodical may be reproduced or transmitted in any form or by any means, electronic or mechanical, including photocopying, recording, or any information storage and retrieval system, without permission in writing from the publisher.

without altering soil structure, and (iii) access limitations or sampling restrictions to sites in protected or sensitive areas. Field infiltration and redistribution experiments are usually based on a larger effective sample size and are therefore preferred for determining the effective properties for a regional-scale model. Pondered infiltration experiments were chosen for this study because they are easy to control and monitor, and yield data relevant at soil water contents all the way up through field saturation.

The widely applied instantaneous-profile method for field determination of soil hydraulic properties (Rose et al., 1965; Vachaud and Dane, 2002; Nimmo and Perkins, 2008) is more suitable for application to plot scales and larger. The method assumes uniform, one-dimensional, downward percolation through a homogeneous porous medium and applies Darcy's law to compute water retention and unsaturated conductivity curves using soil water content and matric pressure data associated with infiltration and redistribution from pondered infiltration. A drawback to this method is that the assumption of vertical flow requires measurements directly below the area of infiltration, normally (if probes are installed vertically) with disruption of the natural layering and structure of the soil being studied. Because of the finite pond size used with infiltration experiments, more lateral spreading is likely than under natural infiltration conditions. Although lateral spreading during pondered infiltration experiments has been well documented (e.g., Glass et al., 2005), subsurface measurements of lateral spreading are typically not made, and it is either ignored or estimated implicitly in the formulas used to calculate soil hydraulic properties.

Analytical solutions can account for spreading (e.g., Reynolds and Elrick, 1990; Nimmo et al., 2008), but must assume some uniform subsurface response that is potentially quite different from the actual response in a heterogeneous natural system. Adjusting the experimental setup to reduce the effect of lateral losses during pondered infiltration is generally not completely effective: installing vertical barriers and increasing the area of infiltration may be genuinely helpful, but the degree and timing of the spreading depends on the soil structure, heterogeneity, and antecedent moisture. For this study, the effects of lateral spreading inherent to pondered infiltration experiments were addressed by estimating effective anisotropies based on soil age.

Effective parameters facilitate quantification of vadose zone fluxes at a scale relevant to the objectives of the given modeling study while still accounting for the effects of heterogeneities at smaller scales than those resolved in the conceptual model (Vereecken et al., 2007). Effective anisotropy includes the influence of multiple thin soil layers that are not considered explicitly in the flow model yet have an effect on lateral fluxes within the system being modeled. Previous studies have investigated the effective anisotropy of unsaturated soils in relation to layering and antecedent soil water content (e.g., Mualem, 1984; Stephens and Heermann, 1988; Yeh et al., 2005). The relation between soil age and the development of well-defined soil horizons for the Mojave site has been characterized by Nimmo et al. (2009).

The fully three-dimensional effects of lateral spreading are difficult to assess in heterogeneous, anisotropic soils using traditional field measurements (e.g., tensiometers for matric pressure and dielectric-constant probes for water content) because the small support volume of most probes requires that a large number of them be installed to accurately quantify spreading. With the

recent application of geophysical methods such as electrical resistivity, it is possible to observe unsaturated zone processes in multiple dimensions with better spatial resolution than can be achieved with a limited number of probes (e.g., al Hagrey and Michaelsen, 1999; Binley et al., 2001; Zhou et al., 2001; Robinson et al., 2003, 2008).

Each of the three soils considered in this study display fundamentally different structures due to varying degrees of pedogenesis, and the infiltration experiments for each soil were made under different initial moisture states (Nimmo et al., 2009). Accounting for the effect of lateral fluxes equally for the three soils therefore required explicit consideration of the spreading with a variety of subsurface measurements in multiple dimensions. Explicit inclusion of the horizontal and vertical dimensions also has practical value in field experiments like those of Nimmo et al. (2009) because the measured data correspond to an inherently multidimensional flow situation.

## Inverse Modeling

Inverse modeling provides the necessary framework for incorporating multidimensional subsurface response data from a variety of measurement techniques (i.e., geophysical and traditional point measurements) into calculations of effective soil hydraulic properties (e.g., Vrugt et al., 2002; Binley and Beven, 2003). When applied to data obtained directly at the scale of interest, inverse modeling can help circumvent many of the issues associated with conventional upscaling methods (Vrugt et al., 2008). The underlying concept of inverse modeling is the iterative adjustment of parameters for a given process model to optimize an objective function. The iterative adjustments typically occur through an automated procedure. The objective function reflects some measure of fit between observed data and their simulated equivalents. The uniqueness of soil hydraulic properties determined via inverse modeling is contingent on the inclusion of both matric pressure and soil water content data in the objective function (Zhang et al., 2003). Given that both inverse modeling and the instantaneous profile method require matric pressure and soil water content data, inverse modeling provides a way to overcome the many limitations of the instantaneous profile method, such as its fundamental one-dimensionality.

Advances in computing power have facilitated an increase in the application of inverse techniques for parameter estimation of soil hydraulic properties in the vadose zone. Previous investigations have applied inverse modeling to a variety of topics in vadose-zone hydrology, including for example: the effect of time-domain reflectometry (TDR) sample volume on estimation of soil hydraulic properties (Schwartz and Evett, 2003); alternate parametric representations of the soil water retention curves (Bitterlich et al., 2004; Lambot et al., 2004); comparison of laboratory-measured vs. inverse-modeled parameters from field experiments (Schwartz et al., 2006); multiobjective inverse modeling for hydraulic properties of layered soils (Mertens et al., 2006); and identifiability of parameters for a dual-permeability model (Kohne et al., 2005). Inverse modeling studies of vadose-zone processes often use one-dimensional flow models and data derived from soil cores or small-scale column experiments, although some studies have considered the importance of multidimensional flow in the field. Ward and Zhang (2007) addressed anisotropy and the spatial variability of soil hydraulic properties for an experimental plot. Yeh et al. (2005) investigated the

three-dimensional nature of anisotropy in natural soils. Reviews by Hopmans and Šimůnek (1999) and Hopmans et al. (2002b) have described the general theory and process of inverse modeling in the vadose zone, while Vrugt et al. (2008) have provided an update of recent progress in inverse techniques and promising approaches, as well as persistent challenges.

### Utility of Effective Soil Hydraulic Properties

Although diffusive flow appears to dominate for the ponded infiltration experiments considered in this study, Nimmo et al. (2009) also observed saturation overshoot and evidence for preferential flow that cannot be completely accounted for by a model based solely on the Darcy–Buckingham–Richards formulation of unsaturated-flow theory. Saturation overshoot occurs when the soil water content at a wetting front temporarily exceeds the quasi-steady water content sustained behind the wetting front by continuation of the applied water flux (Stonestrom and Akstin, 1994; DiCarlo, 2004; Nimmo et al., 2009). Besides these anomalous flow phenomena, a major obstacle to accurately matching point measurements in highly heterogeneous field sites—like those considered in this study—with simulations based on Richards' equation is acquiring sufficient data to characterize the spatial variations in the porous media properties, particularly in the horizontal direction. Although it is clear that horizontal heterogeneity affected the observed probe responses for all three soils considered in this study (Nimmo et al., 2009), no data exist to quantitatively characterize such variability.

Numerical simulations based on Richards' equation and other relatively simple approaches are routinely applied to situations that are fundamentally more complex than the data intrinsically represent (e.g., Baveye et al., 2002; Hopmans et al., 2002a; Pachepsky et al., 2006). The objectives of any modeling study define the scales of interest, which in turn dictate the level of heterogeneity that is explicitly represented vs. that which must be accounted for by effective parameters of the model (Vereecken et al., 2007). Indeed, any distributed model should be used with the understanding that (i) the model quantifies a subset of the known phenomena, (ii) the model parameters are assigned effective values across a defined support volume, and (iii) the results must be considered as an effective representation of more complex processes. For example, in the context of this study, a saturated hydraulic conductivity determined by inverse modeling is a parameter value selected on the criterion that it allows an inherently oversimplified flow model of the infiltration experiment to most closely match the observed results. Thus, the criterion for justifying (or rejecting) an approach based on Richards' equation is not its formal physical validity but rather whether its results can provide an adequate and useful quantitative description of the natural flow processes, including those not formally represented in the model (National Research Council, 2001, p. 31). This study included a comparative test based on this criterion that compared inverse modeling results with an independent set of electrical resistance imaging (ERI) data. With the understanding that the model applied cannot fully represent the physical situations modeled, simulation results were then judged on the basis of their adequacy to make predictions useful for the purpose at hand.

### Materials and Methods

Three ponded infiltration experiments were performed in the Mojave National Preserve (Nimmo et al., 2009) at locations

selected to represent the range of observed pedogenic development for the Mojave Desert: (i) recently deposited sediments in an active wash, (ii) a soil of early Holocene age, and (iii) a highly developed soil of late Pleistocene age. For all three experiments, a 1.0-m-diameter circular concrete ring was cast in place to seal it to the soil and confine the infiltration area. Sustained ponding through regular application of water maintained a relatively constant head for approximately 2.5 h (Table 1). The estimation of effective soil hydraulic properties with inverse modeling presented here used the volumetric measurements of applied water and the response data from a multidimensional array of tensiometers and dielectric-constant probes during infiltration and redistribution. Electrical resistance imaging during infiltration and redistribution, and core samples from various depths adjacent to the infiltration experiments, were not available for all three soils. Electrical resistance imaging for the active wash deposits and Pleistocene soil and core-sample data for the active wash and Holocene soil were used as a qualitative comparison against the results but were not considered explicitly in the inverse modeling. The variety in the types of data available for this study provided a robust foundation for both parameter optimization and the evaluation of modeling results.

### Numerical Models

The flow model VS2D (Lappala et al., 1987; Hsieh et al., 2000) was selected for its ability to simulate variably saturated subsurface flow in multiple dimensions. The VS2D model solves the two-dimensional approximation of Richards' equation through time using the finite-difference method and is capable of solving systems in radial coordinates, thus allowing a quasi-three-dimensional representation of a system (assuming angular symmetry). The heat and solute transport capabilities of VS2D were not applied in this study. The VS2D code allows selection of several parametric representations of the water-retention curve (i.e., Brooks and Corey, Haverkamp, and van Genuchten), but it was modified for this study to incorporate the Rossi and Nimmo (1994) junction model (R. Healy, written communication, 2006), which provides a more realistic relation in the dry range. The water retention and hydraulic conductivity relation used in VS2D is based on Mualem (1976). An added advantage of VS2D is that it can be easily integrated with the widely available universal inverse code UCODE\_2005 (Poeter et al., 2005). The UCODE\_2005 (henceforth referred to simply as UCODE) was used for sensitivity analysis and parameter estimation.

The modified Rossi and Nimmo (1994) version of VS2D has six physical parameters for each hydrogeologic unit: effective porosity,  $n_e$  ( $\text{m}^3 \text{m}^{-3}$ ), horizontal saturated hydraulic conductivity,  $K_h$  ( $\text{m s}^{-1}$ ), anisotropy ratio,  $K_z/K_h$  (dimensionless), specific storage,  $S_s$  ( $\text{m}^{-1}$ ), and the two Rossi–Nimmo parameters, the matric-pressure scaling factor  $\psi_o$  (m water) and the curve-shape parameter  $\lambda$  (dimensionless). For this study, soil water content was set to zero at a matric pressure of  $-10^5$  m water (Ross et al., 1991; Rossi and Nimmo, 1994) and specific storage was set equal to zero.

### Flow Model Scenarios

The conceptual model of flow was represented by three VS2D scenarios—one for each infiltration experiment. The scenarios were designed to minimize boundary effects and computational expense of the simulations while still representing the relevant

TABLE 1. Characterization of the VS2D simulation scenarios, including applied flux boundary condition, fixed parameters, initial conditions, and inverse-estimated mean effective parameter values.

Parameter	Active wash	Holocene soil	Pleistocene soil
<b>Applied flux†</b>			
Rate, $m\ s^{-1}$	$2.20 \times 10^{-4}$	$1.25 \times 10^{-4}$	$4.78 \times 10^{-5}$
Duration, h	2.41	2.63	3.00
<b>Fixed parameters‡</b>			
$K_z$ , $m\ s^{-1}$	$3.52 \times 10^{-4}$	$2.00 \times 10^{-4}$	$7.65 \times 10^{-5}$
$n_e$ , $m^3\ m^{-3}$	0.3	0.35	0.50 (upper), 0.35 (lower)
<b>Initial conditions§</b>			
$\theta_1$ , $m^3\ m^{-3}$	0.02	0.02	0.05
$\theta_2$ , $m^3\ m^{-3}$	0.05	0.05	0.10
$\theta_3$ , $m^3\ m^{-3}$	0.07	0.10	0.15
<b>Optimized parameters¶</b>			
<b>Upper hydrogeologic unit</b>			
$K_h$ , $m\ s^{-1}$	$8.0 \times 10^{-3}$ ( $4.3 \times 10^{-3}$ )	$3.0 \times 10^{-4}$ ( $3.5 \times 10^{-5}$ )	$2.4 \times 10^{-4}$ ( $1.5 \times 10^{-4}$ )
$\lambda$	2.72 (0.41)#	5.46 (1.66)#	0.32 (0.09)
$\psi_o$ , -m	0.06 (0.01)#	0.28 (0.05)#	0.32 (0.10)
$K_h/K_z$	22.7 (12.22)	1.5 (0.18)	3.1 (1.96)
<b>Lower hydrogeologic unit</b>			
$K_h$ , $m\ s^{-1}$	$7.5 \times 10^{-5}$ ( $7.6 \times 10^{-5}$ )	$2.2 \times 10^{-1}$ ( $1.6 \times 10^{-1}$ )	$3.8 \times 10^{-4}$ ( $3.5 \times 10^{-4}$ )
$\lambda$	2.72 (0.41)#	5.46 (1.66)#	8.61 (2.68)
$\psi_o$ , -m	0.06 (0.01)#	0.28 (0.05)#	1.61 (0.10)
$K_h/K_z$	0.2 (0.22)	$1.1 \times 10^3$ ( $8.0 \times 10^2$ )	5.0 (4.58)
Number of included sets††	75	150	20

† Equal to the mean rate measured by Nimmo et al. (2009).

‡  $K_z$ , vertical saturated hydraulic conductivity, set equal to 1.6 times the applied flux rate;  $n_e$ , effective porosity, set equal to 75% of maximum observed water content for each hydrologic unit.

§ Initial soil volumetric water content values ( $\theta$ ) for flow simulations.

¶ Mean parameter values and standard deviations (in parentheses), calculated using parameter sets that meet the inclusion criteria:  $K_h$ , horizontal saturated hydraulic conductivity;  $\lambda$ , water retention curve shape parameter (Rossi and Nimmo, 1994);  $\psi_o$ , water retention curve shape parameter (Rossi and Nimmo, 1994);  $K_h/K_z$ , anisotropy ratio.

# For the active wash and Holocene soil, single Rossi–Nimmo parameter values were optimized and assigned for the entire domain.

†† Number of parameter sets included in the calculation of mean parameter value and standard deviation.

features of the natural system and realistic wetting front propagation. For consistency, a number of characteristics were common to all simulation scenarios, each of which (i) solved Richards' equation in cylindrical coordinates, with angular symmetry centered at the middle of the infiltration ring, (ii) utilized an adaptive time step, with output times corresponding to probe and ERI sampling intervals, (iii) had domain dimensions of 2.0-m depth and 5.0-m radius (Fig. 1), (iv) used the same finite-difference mesh spacing with variable vertical and horizontal discretization ranging from 0.01 by 0.01 m in the near surface underneath the infiltration zone to 0.04 by 0.10 m at depth near the outer edges of the domain (Fig. 1a), and (v) shared the same boundary conditions of no-flow sides, a seepage face along the base, an applied flux across the infiltration zone for the duration of the infiltration experiment (Table 1), and a no-flow boundary across the rest of the surface (Fig. 1).

The applied flux boundary condition was used instead of a constant head because the volumetric flux applied was known more precisely than the level in the infiltration pond (Nimmo et al., 2009). Additionally, an applied flux is advantageous because it ensures an exact mass balance, regardless of the accuracy of the inverse modeling. Although the measured infiltration rates for the three experiments fluctuated slightly through time (Nimmo et al., 2009), the variability was minor and the assumption of a constant rate of applied flux for the duration of infiltration was acceptable. The constant rate applied in each scenario was set equal to the mean observed infiltration rate for the experiment (Table 1),

which assumes immediate steady infiltration and ignores the falling head at the end of infiltration. Immediate application of the mean infiltration rate is justifiable because the sampling interval of the probes (600 s) was longer than the time to reach steady infiltration for all three experiments. It should also be noted that prior VS2D simulations across a feasible parameter range confirmed that the depth and width of the finite difference meshes were sufficiently large to eliminate effects of the bottom and side boundary conditions on wetting front propagation.

The complexity of the conceptual flow models was restricted by both data availability and the need to maintain appropriate parsimony of the inverse problem (Hill and Tiedeman, 2007). The domain of each VS2D scenario was divided into upper and lower hydrogeologic units (Fig. 1). Although several layers were visible within all three soil ages (Nimmo et al., 2009), the definition of two hydrogeologic units for the conceptual model of flow emphasizes the sharpest textural contrast between layers observed at each experiment location. The inverse-estimated parameters will ultimately be applied to a regional-scale model of soil moisture dynamics,

which, due to computational expense, would also represent complex soil horizons as two-layer systems of uniform thickness.

### Defining the Objective Function

For each scenario, UCODE automated a series of forward runs for the flow model and compared field observations with their simulated equivalents at every iteration to minimize the objective function:

$$O(P) = \sum_{i=1}^n w_i [o_i - s_i(P)]^2 \quad [1]$$

where  $P$  is the set of forward-model parameters,  $o_i$  are the observed values and  $s_i$  the corresponding values simulated with parameter set  $P$ ,  $n$  is the total number of observations, and  $w_i$  are the weights associated with observations  $o_i$ . With each iteration, UCODE calculates the sensitivities of simulated data to the model parameters by perturbing parameters individually in a series of forward runs, one for each parameter, and then adjusts the parameter values from the previous iteration and updates the objective function. The UCODE terminates when the best-fit parameter set is reached, as determined by the user-defined convergence criteria. The UCODE default convergence criteria are met when, for two sequential iterations, each parameter in set  $P$  changes in magnitude by <1%.

The field data (Nimmo et al., 2009) used to inform Eq. [1] were matric pressures from tensiometers and water contents from two types of dielectric-constant probes: (i) TDR waveguide pairs

and (ii) EC-20 probes (Decagon Devices, Pullman, WA). The weights ( $w_i$ ) in Eq. [1] reflect the relative uncertainty of the observations ( $o_i$ ) and were calculated assuming variances based on a lognormal distribution in measurement error, given the manufacturers' reported measurement error:  $\pm 4\%$  in volumetric water content ( $\text{m}^3 \text{m}^{-3}$ ) for the EC-20,  $\pm 2.5\%$  in volumetric water content ( $\text{m}^3 \text{m}^{-3}$ ) for the TDR probes, and  $\pm 0.05 \text{ m}$  in matric pressure for tensiometers. Although each of these measurement types also has a distinct support volume, this volume may vary depending on both the experiment location and the depth within a given soil profile. For this work, each probe was treated as a point measurement, with simulated observation node locations corresponding to the midpoint of each probe (Fig. 1). An additional nuance of the multidimensional array of point measurements is related to the assumption of angular symmetry applied to the conceptual model, where measurements from two axial transects (Nimmo et al., 2009) were collapsed into one plane. Probe holes D, E, and F are from one axial transect, while G, H, and I are from a perpendicular transect; these probe holes were co-located in pairs D/G, E/H, and F/I for the VS2D scenarios (Fig. 1a).

### Initial Conditions

Measurements of soil water content ( $\theta$ ) and matric pressure ( $\psi$ ) before the onset of infiltration indicated a greater degree of heterogeneity in the porous media than could reasonably be considered given the simplification of the process model simulations. The initial conditions of each VS2D simulation scenario must be consistent with the initial probe readings, however, to achieve a reasonable match between subsequent probe measurements and simulated output. The measurements of initial  $\theta$  varied in space without correlation to location within the soil profile. For each experiment location, however, the magnitude of all initial  $\theta$  measurements was approximately equal to one of three values (Table 1). Every UCODE iteration considered these different initial conditions separately by performing three sequential forward runs of the process model, all with the same overall parameterization but each with a different initial  $\theta$  value applied to the entire simulation domain. In Eq. [1], simulated output from each of the three forward runs is compared with the observations from

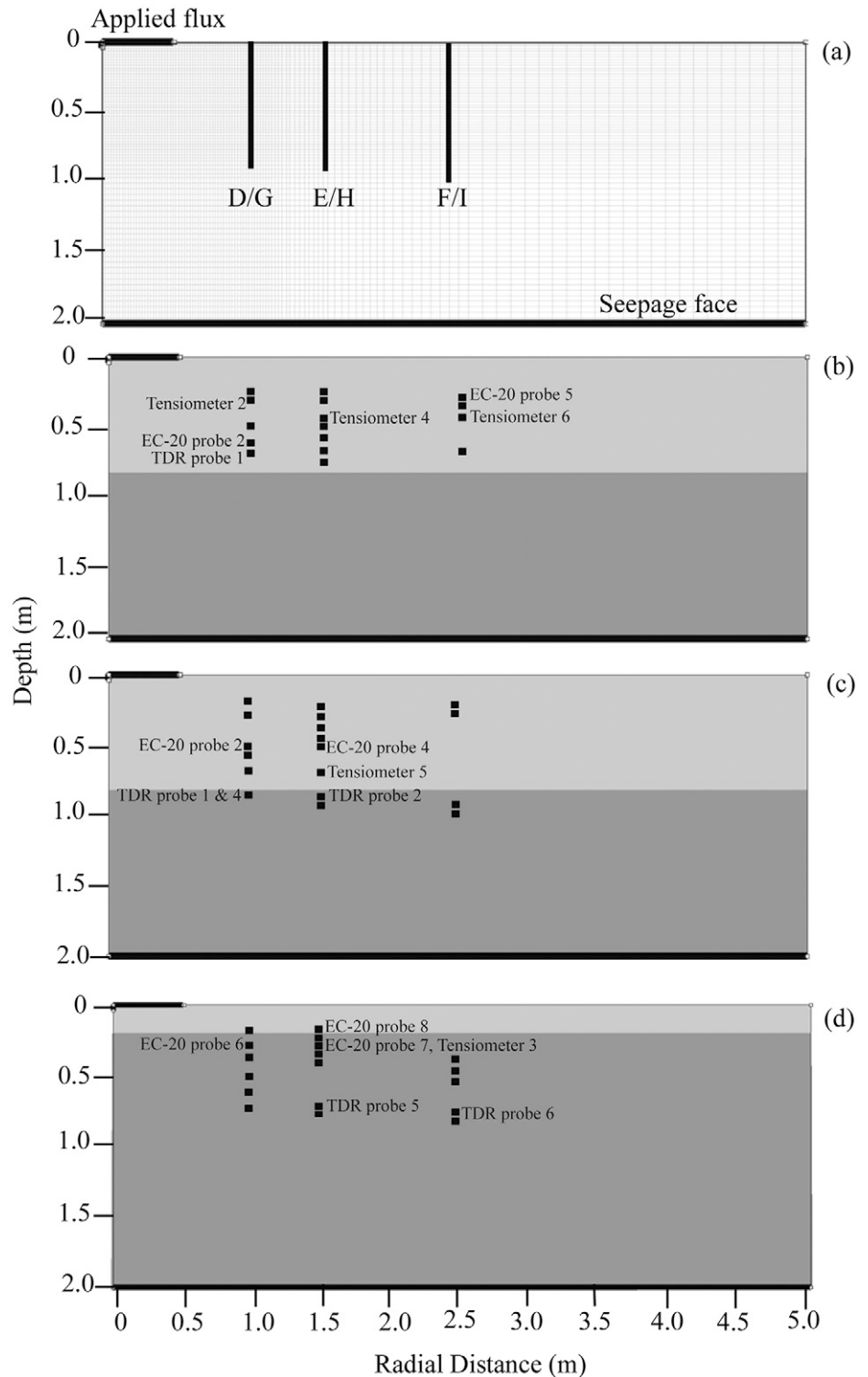


FIG. 1. Characteristics of the VS2D simulation domains: (a) finite-difference mesh with boundary conditions labeled (all unlabeled boundaries are no flow); probe locations and position of hydrogeologic units shown in light gray (upper unit) and dark gray (lower unit) for: (b) the active wash, (c) the Holocene soil, and (d) the Pleistocene soil. Probe-hole locations are: D/G at 0.5 m, E/H at 1.0 m, and F/I at 2.0 m from the edge of the infiltration pond; EC-20 and TDR are dielectric constant probes for water content.

the subset of probes with the same measured value of initial  $\theta$  as was assigned for the simulation. Simulations and the observations are therefore only compared if they share roughly the same initial  $\theta$  values. In VS2D it is not possible to define initial  $\psi$  and  $\theta$  independently. Instead, the initial distribution of  $\psi$  was defined by the

corresponding value of  $\theta$  from the water-retention curve applied for the given forward run. Tensiometer measurements were compared to output from all forward runs in the inversion.

### Parameter Sensitivity and Optimization

Parameter estimation was considered in the same way for all three experiment locations, with exceptions noted below. Previous measurements at the Mojave field site by Nimmo et al. (2008, 2009) and some reasonable assumptions regarding the conceptual model of the flow system facilitated a reduction in the number of parameters considered in the inverse problem (Eq. [1]), thus increasing computational efficiency. For example, effective porosity  $n_e$  was fixed at 75% of the maximum observed water content for each hydrogeologic unit, equivalent to assuming that, under conditions of field saturation, 25% of the pore space is occupied by trapped air, as is consistent with empirical trends for desert deposits similar to those considered in this study (Winfield et al., 2006). These fixed porosity values additionally agree with gravimetric measurements on core samples from the active wash deposits and the Holocene soil (no core was taken from the Pleistocene soil). Table 1 lists the relevant VS2D parameters that were fixed for the inverse problem. It should be noted that although the denominator of the anisotropy ratio was fixed (i.e., vertical saturated hydraulic conductivity) for the inversion based on the observed infiltration rates (Nimmo et al., 2008, 2009), the numerator was allowed to vary through consideration of horizontal saturated hydraulic conductivity (Table 1).

Parsimony of the inverse problem was enhanced using preliminary sensitivity analysis to further reduce the number of parameters considered. The results of these preliminary sensitivity analyses are described below, and the final group of parameters optimized in the inversions for each VS2D scenario is given in Table 1. Parameters with low sensitivities and high correlation coefficients indicate that the observed data do not support independent estimation of their values. Due to the lack of data in the lower hydrogeologic units for the active wash (Fig. 1b) and the Holocene soil (Fig. 1c),  $\psi_o$  and  $\lambda$  in the lower unit for these two experiment locations had low sensitivities and were highly correlated with each other. In the Pleistocene soil, the majority of the observations were in the lower hydrogeologic unit (Fig. 1d), which explains higher sensitivities and lower correlations for  $\psi_o$  and  $\lambda$  relative to the other two experiment locations. Thus for the Pleistocene soil,  $\psi_o$  and  $\lambda$  for the upper and lower units were considered independently, whereas for the Holocene soil and active wash, single values of  $\psi_o$  and  $\lambda$  were optimized for the entire domain (Table 1). Sensitivity analysis showed that the horizontal saturated hydraulic conductivity ( $K_h$ ) of the lower unit had a high sensitivity for all experiment locations. Due to its coupling to vertical saturated hydraulic conductivity ( $K_z$ ) through the anisotropy ratio,  $K_h$  affects spreading in the lower unit and influences the rate at which water can percolate out of the upper unit. Thus  $K_h$  was considered in the inversion for both units at all three experiment locations (Table 1).

Each UCODE run requires initial values for the parameters of interest. As UCODE uses a local search method in minimizing the objective function (Eq. [1]), the initial parameterization can influence the success of the inversion. Laboratory analysis of core samples or soil texture measurements (Nimmo et al., 2009) provided an expected range of parameter values for each

site independent from the infiltration experiments and a starting point for UCODE parameter estimation runs. Using initial values from this range tended to reduce the number of iterations necessary for each UCODE run by improving the process-model fit, as determined by the standard error of regression (SER), which is calculated by

$$SER(P) = \sqrt{\frac{1}{n-K} \sum_{i=1}^n [o_i - s_i(P)]^2} \quad [2]$$

where  $n$  is the number of observations and  $K$  is the number of parameters within parameter set  $P$  that are estimated. The SER is a useful metric for determining whether the iterations are improving the process-model fit (Hill and Tiedeman, 2007).

The extreme nonlinearity of the forward and inverse models considered here resulted in objective functions with multiple local minima and a distinct lack of any global minimum. Despite numerous attempts with different initial parameter sets, the default UCODE convergence criteria were not met for any of the three experiment locations. When the default convergence criteria are not met, UCODE continues to run until it performs the user-specified maximum number of iterations. Results from selected nonconvergent UCODE runs revealed that some initial parameterizations produced a much better process-model fit than others; for some of the inverse runs, the SER reached a distinct minimum value for each experiment location (Fig. 2). Regardless of the lack of convergence, correlations between all parameters considered were  $<0.95$ , indicating that the individual parameters were being optimized and not the ratio of one parameter to another (Hill and Tiedeman, 2007). Thus, while there is not a unique, best-fit parameter set for any of the three simulation scenarios, all parameter sets associated with the minimum SER value for a given scenario represent an equally good degree of process-model fit.

Rather than further constrain the VS2D scenarios or loosen the UCODE-defined convergence criteria, the results of the nonconvergent UCODE runs were interpreted in a probabilistic manner. To replace the convergence criteria, a new inclusion criterion was established to develop probability distributions of the expected parameter values. Different initial parameter values were used in multiple UCODE runs for each experiment location. Every set of parameter values from any UCODE iteration reaching the minimum SER was deemed an equally likely parameter set for achieving the best possible model fit. Parameter sets were not considered from inversions in which the minimum SER was never reached. The VS2D simulations were more computationally expensive for the Pleistocene soil, and UCODE required two additional forward runs of VS2D for each iteration because  $\psi_o$  and  $\lambda$  values were optimized for both the upper and lower hydrogeologic units (Table 1). To increase computational efficiency and avoid the possibility of VS2D becoming numerically unstable during the later inverse iterations for the Pleistocene soil, UCODE was run with fewer sequential iterations than for the active wash and Holocene soil. Nonetheless, the minimum SER value was still reached in the runs with fewer iterations (Fig. 2).

## Results and Discussion

Probability distributions of horizontal saturated hydraulic conductivity ( $K_h$ ) values from parameter sets meeting the inclusion criteria are shown in Fig. 3; mean values and standard

deviations of each hydrogeologic unit for the different soil ages are given in Table 1. The average  $K_h$  of the upper unit is much greater for active wash deposits than for both the more developed Pleistocene soil and the Holocene soil, which have  $K_h$  within an order of magnitude of each other (Fig. 3a). This result is supported by the observed probe response timing and measured infiltration rates at the three experiment locations (Nimmo et al., 2009). The lower unit  $K_h$  shows a different trend, with the active wash displaying the lowest mean conductivity and the Holocene soil the highest (Fig. 3b). It is more difficult to interpret these results for the lower unit due to the fixed  $K_z$  applied at all three experiment locations. The substantially larger  $K_h$  value for the lower hydrogeologic unit of the Holocene soil and the correspondingly large anisotropy ratio indicate that a greater degree of lateral subsurface spreading occurred at depth for this soil age.

Probability distributions of the two Rossi and Nimmo (1994) parameters are shown in Fig. 4, and indicate a distinct variation between water-retention properties of the different soil ages. In particular, a less negative  $\psi_o$  (Fig. 4a) corresponds to greater  $K_h$  in the upper hydrogeologic unit (Fig. 3). Figure 5 shows the Rossi–Nimmo retention curves calculated using mean inverse-estimated parameter values from each experiment location (Table 1). For the 0.05-m-diameter core samples taken from the active wash deposits and Holocene soil, retention data were measured using the method of Constantz and Herkelrath (1984), and are plotted as points on Fig. 5a and 5b. For the Pleistocene soil, collocated tensiometer and TDR measurements at 0.60-m depth are plotted as points in Fig. 5c. For all modeled retention curves, the matric pressure value that corresponds with  $\psi_o$  becomes more negative with increasing soil age (Fig. 5). The much gentler slope of the water-retention curve for the upper hydrogeologic unit of the Pleistocene soil is a result of its lower  $\lambda$  values (Fig. 5).

The apparent differences between the overall shape of the observed and modeled retention curves are due in part to the simplifying assumptions applied to the inverse problem. The observed and modeled curves are also estimated across different scales, however: the modeled results effectively represent the entire volume of the hydrogeologic unit that was influenced by the infiltrated water, whereas the measured results represent an individual core-sample volume. For the active wash (Fig. 5a), the minor differences between observed and modeled curves can be mostly accounted for by slight differences in porosity and specific storage values, which would shift the wet and dry ends of the curve. The Holocene soil (Fig. 5b) shows greater and more systematic variation of lab-measured values with depth than does the active wash. The inverse modeled curve for the Holocene soil (Fig. 5b) also has a greater value of  $\lambda$  than those

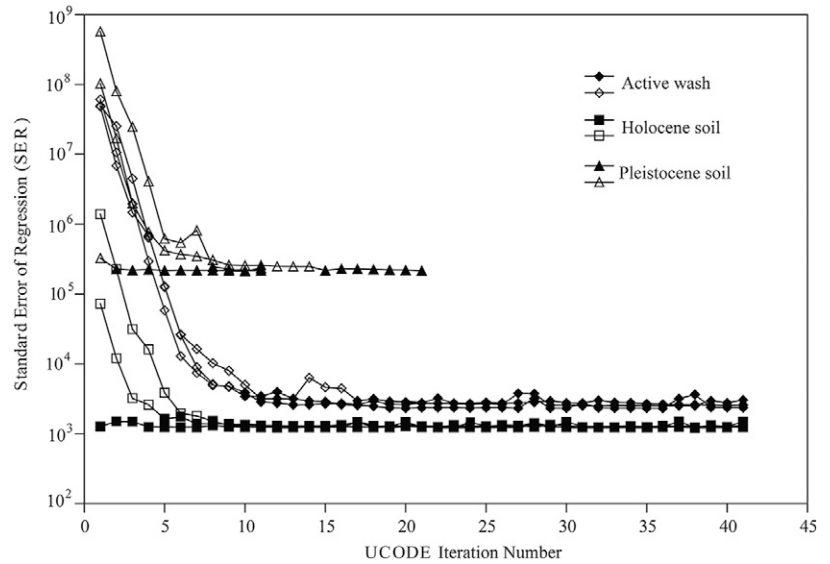


FIG. 2. Standard error of regression (SER) plotted against number of iterations of the process model for three selected nonconvergent UCODE runs for each experiment location. Iterations reaching the minimum SER are plotted as filled symbols, other iterations are plotted as open symbols.

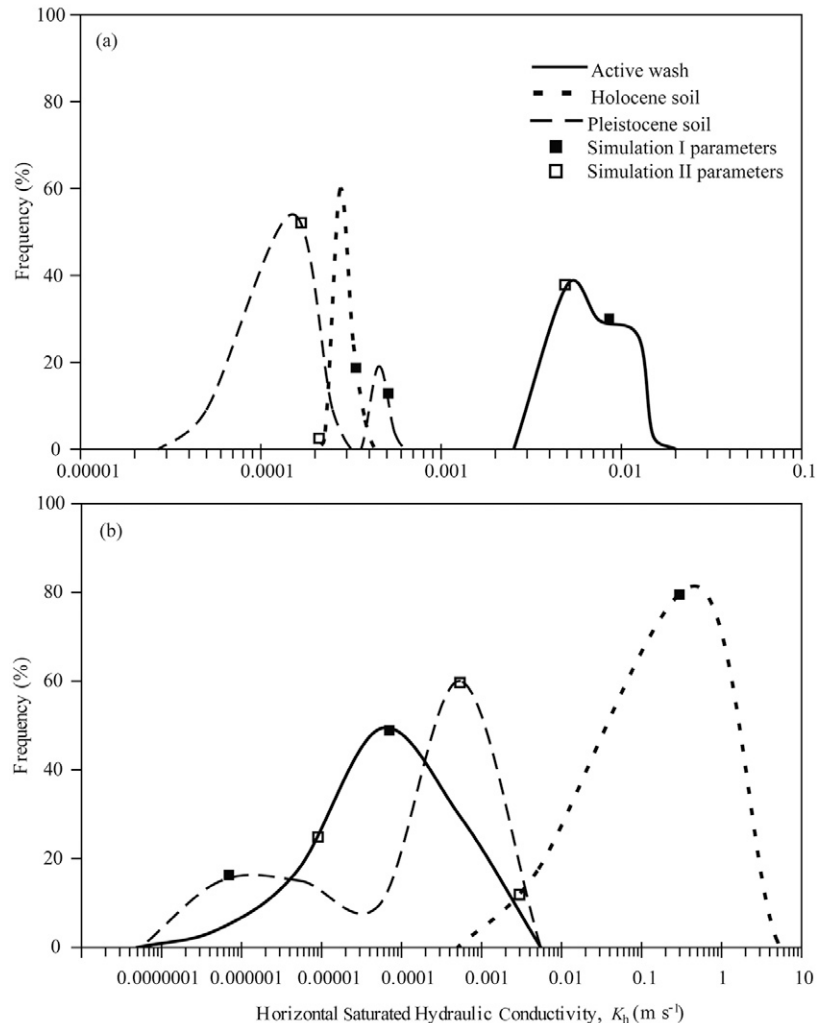


FIG. 3. Probability distributions for horizontal saturated hydraulic conductivity in the (a) upper and (b) lower hydrogeologic units for parameter sets meeting the inclusion criteria at all three experiment locations; values from two representative parameter sets for illustration of forward model simulations are indicated by the square symbols.

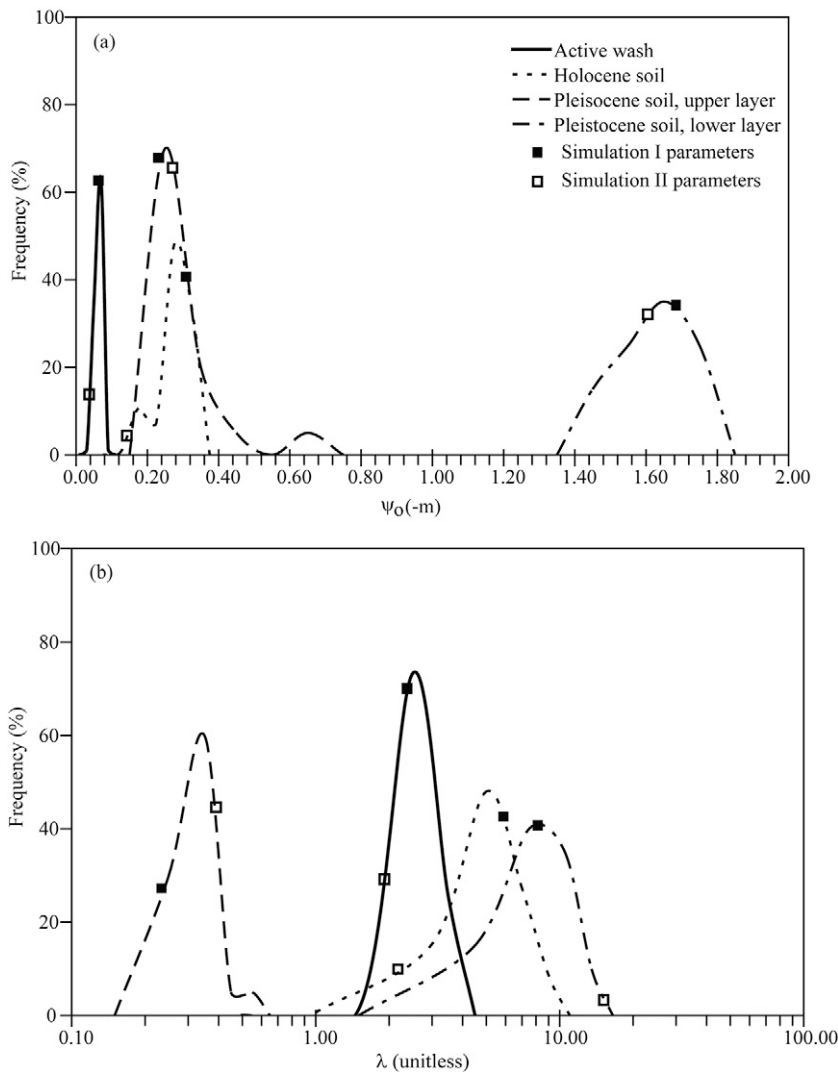


FIG. 4. Probability distributions for Rossi–Nimmo water retention curve shape parameters (a)  $\psi_0$  and (b)  $\lambda$  for both hydrogeologic units for parameter sets meeting the inclusion criteria at all three experiment locations; values from two representative parameter sets for illustration of forward model simulations are indicated by the square symbols.

determined from any of the measured results. The simultaneous point measurements from the Pleistocene soil (Fig. 5c) require a Rossi–Nimmo curve with an even more negative  $\psi_0$  and a smaller  $\lambda$  than the modeled curve for the lower unit.

Overall, the retention curves estimated with the inverse approach typically have larger  $\lambda$  and more negative  $\psi_0$  values than curves that the measured values would produce (Fig. 5). Similarly, when compared with other core-scale measurements of desert soil hydraulic properties (Winfield et al., 2006), the inverse-modeled  $\lambda$  values are greater and  $\psi_0$  are more negative for the curves estimated in this study. This trend in inverse-estimated Rossi–Nimmo curve parameter values is probably related to the greater degree of heterogeneity, soil structure, and flow processes not represented by Richards' equation that are lumped into these effective parameters. Still, the curves derived through inverse modeling show a similar trend with age. Across all three experiment locations, the parameter values estimated by UCODE are within a physically reasonable range for desert soils (Winfield et al., 2006).

The UCODE-calculated SER values (Eq. [2]) in Fig. 2 provide a quantitative measure of the goodness of fit between the observed and simulated response to infiltration for the three sites. Visual comparison of simulation results with the field observations is useful to further assess model performance related to the magnitude and timing of the response. Figures 6 to 8 show the results from representative forward simulations of VS2D with parameter sets meeting the inclusion criteria. Two parameter sets (Simulations I and II) were selected for each experiment location to represent the range in the optimized probability distributions (Fig. 3 and 4). Figures 6 to 8 compare the results from Simulations I and II with the corresponding observations for six selected probes from each experiment, with locations shown in Fig. 1. The six simulated outputs were selected to illustrate the range of process model performance and, therefore, include both the best and worst fits for each soil age. For all three experiments, there was no apparent correlation between probe location and the quality of process model fit.

The simulation for the active wash displays a reasonably good match with the observed response (Fig. 6), although a few probes are poorly simulated (e.g., Fig. 6f). The process model mimics the nonresponsive probes (e.g., Fig. 6b) and the timing of increases and decreases in  $\psi$  and  $\theta$  of the responding probes (e.g., Fig. 6a, 6c, 6d, and 6e). In general, the model does a good job of simulating the magnitude of either the early response (e.g., Fig. 6d) or the temporal change during redistribution (e.g., Fig. 6a, 6c, and 6e), but not both. The simulations of the Holocene soil generally show good agreement with the magnitude and timing of the probe response to infiltration and redistribution (Fig. 7). The simulations mimic the

nonresponsive probes (e.g., Fig. 7b) and a few of the simulated equivalents match the observed response in terms of timing and magnitude (e.g., Fig. 7d). Other simulated probe equivalents match the observed timing well but not the magnitude (e.g., Fig. 7f), or are accurate in magnitude for only the early response (e.g., Fig. 7e) or during redistribution (e.g., Fig. 7c) but not both. Additionally, some simulations do a reasonable job of depicting the magnitude but not the timing during the early response (e.g., Fig. 7a). Agreement between observations and their simulated equivalents is the worst for the well-developed Pleistocene soil (Fig. 8). Generally, simulations for the Pleistocene soil either greatly underestimate (e.g., Fig. 8a) or slightly overestimate (e.g., Fig. 8b, Simulation I) the magnitudes of probe responses. The forward runs for the Pleistocene soil reasonably simulate some of the nonresponding probes (e.g., Fig. 8c–8e); however, they do not reproduce the irregular response pattern at this experiment location (e.g., Fig. 8f).

Figures 9 and 10 show measured changes in resistivity for both the active wash and the Pleistocene soil, adjacent to

corresponding snapshots of simulated water content from one representative parameter set. The representative parameter sets used for the simulations correspond to the Simulation I values for  $K_h$ ,  $\psi_o$ , and  $\lambda$  shown in Fig. 3 and 4. Unless there are changes in the salinity of the system during the course of the experiment, decreases in resistivity should correspond to increases in soil water content. Due to the experimental setup and the physics of resistivity measurements, there is essentially no sensitivity in the lower corners of the domain, and the maximum depth of ERI sensitivity is just over 1 m. For consistent comparison with the ERI results in Fig. 9 and 10, the VS2D-simulated outputs are shown with mirror images on the left-hand side to reflect the symmetry around the infiltration pond (in the center of the domain) and truncated to show only the upper 1.2 m of the simulated domain.

The simplifying assumptions regarding heterogeneity and initial conditions do not apply equally well to the three experiment locations. This is reflected by both the variability between the minimum SER (Fig. 2) and the disparate quality of fit between the observed  $\theta$  and  $\psi$  to simulated equivalents (Fig. 6–8) for the three experiment locations. This discrepancy is particularly obvious for the Pleistocene soil (Fig. 8 and 10) and is probably due to the well-developed, fine-textured, vesicular Av horizon and strong heterogeneity within the other soil layers (Nimmo et al., 2009) that was not considered explicitly in the process model representation of this soil. Conversely, for the Holocene soil (Fig. 7), large effective anisotropies allow the simplified process model to adequately represent the effect of multiple soil layers on lateral spreading.

The use of the resistivity results in optimizing parameters would require an inversion that includes the ERI data explicitly, perhaps by converting the changes in modeled water content to changes in electrical resistivity and predicting the changes in measured voltage for use in optimization. This step is not trivial, however, given the rock physics relations required and issues with parameterization and data weighting of this data set. Consequently, the possibility of solving a coupled inverse problem using ERI as well as probe data remains for a later study, and the ERI inversions were used here only to qualitatively evaluate the success of the inversion and data analysis as presented above. Comparisons of ERI with simulated snapshots using one of the equally likely parameterizations of VS2D (Fig. 9 and 10) show that the shape and timing of the wetting front development and redistribution match very well for the active wash, although not as well for the Pleistocene soil. For the Pleistocene soil, using a model with a greater number of hydrogeologic units might decrease the rate at which the simulated wetting front propagates downward and produce a better qualitative match to the ERI. Such a formulation of the process model would be consistent with the more complex stratigraphy observed at this experiment location (Nimmo et al., 2009). For neither the active wash nor the Pleistocene soil do the homogeneous hydrogeologic units of the simulations express the degree of local variations captured by ERI.

### Discussion

This work presents an inverse modeling framework using UCODE together with VS2D to incorporate the inherent effects of lateral spreading during ponded infiltration into soil hydraulic property estimation. The method was used to constrain physical

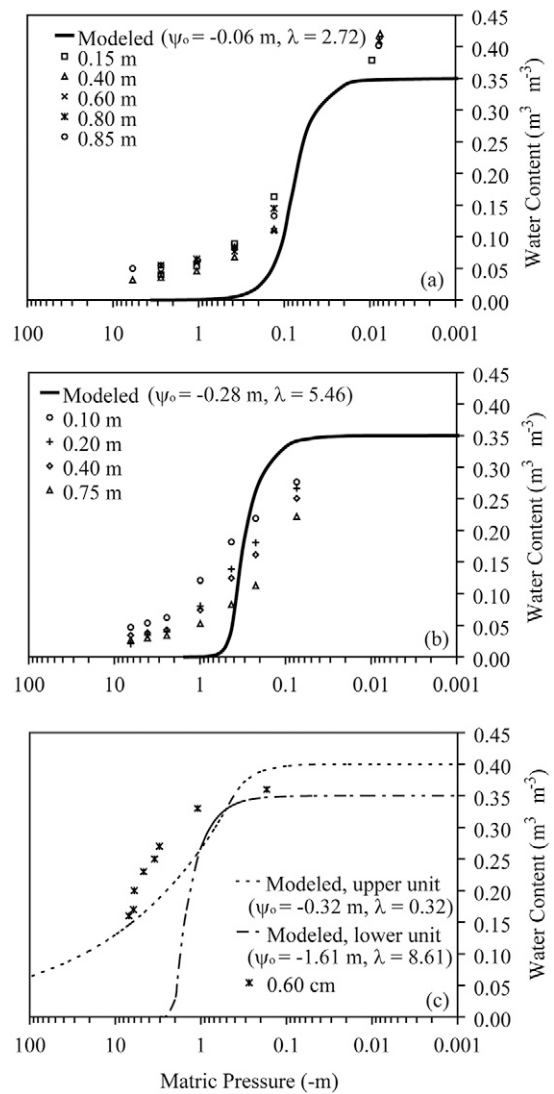


FIG. 5. Example soil water retention curves using the mean inverse-estimated values of the Rossi–Nimmo water retention curve shape parameters  $\psi_o$  and  $\lambda$  given in Table 1 for: (a) the active wash; (b) the Holocene soil; and (c) the Pleistocene soil. Laboratory measurements from soil cores collected from variable depths within the upper hydrogeologic unit are plotted for the active wash and Holocene soil. Simultaneous measurements of matric pressure and water content from co-located probes in the lower hydrogeologic unit of the Pleistocene soil are also plotted.

parameters based on soil age and texture for future application to a dynamic soil moisture model of large portions of the Mojave Desert. One virtue of this approach over commonly used field techniques for estimating unsaturated hydraulic properties is that it is not strictly limited to particular simplified conceptual models of the subsurface. By using a two-dimensional numerical model together with spatially distributed subsurface measurements, this approach does not require generalized assumptions about a postulated degree of spreading, as in certain other methods of calculating ring infiltrometer results (e.g., Nimmo et al., 2008). Given information about subsurface layering and texture, this approach can be applied consistently to widely varying soil types. Other benefits include: (i) this approach explicitly considers anisotropy, which is an inherent characteristic of any naturally stratified system such as soil, and (ii) multiple data types for both

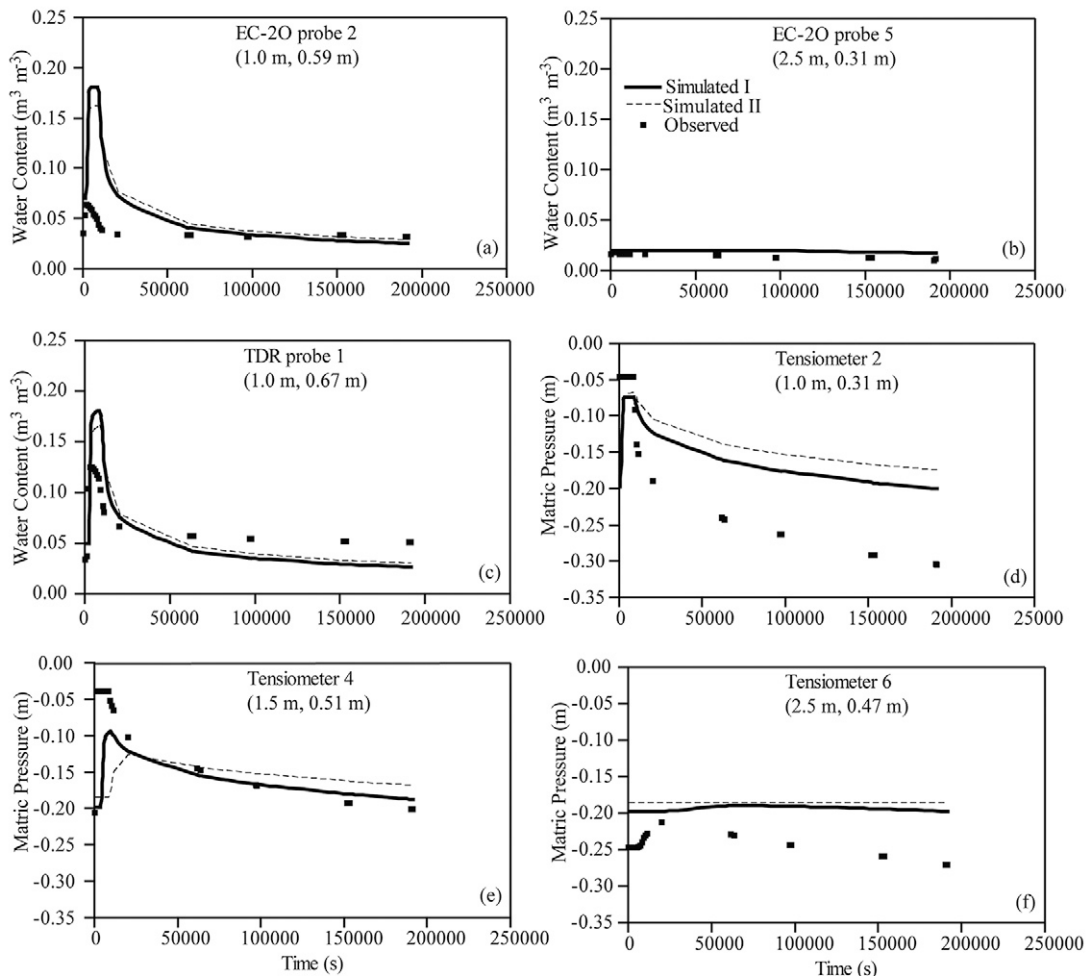


FIG. 6. Time series of observations from selected EC-20 and TDR dielectric constant probes for water content and tensiometers vs. two simulated responses for the active wash. Coordinates of probe placements (radial distance from center of infiltration pond, depth from surface to middle of probe) are given for: (a) EC-20 Probe 2; (b) EC-20 Probe 5 (best fit); (c) TDR Probe 1; (d) Tensiometer 2; (e) Tensiometer 4; and (f) Tensiometer 6 (worst fit). Parameter values used for Simulations I and II, respectively, are: horizontal saturated hydraulic conductivity  $K_h$  (upper unit) =  $1.3 \times 10^{-2}$  and  $4.9 \times 10^{-3} \text{ m s}^{-1}$ ; Rossi-Nimmo water retention curve shape parameters  $\psi_o = 0.06$  and  $0.04 \text{ -m}$  and  $\lambda = 2.27$  and  $1.83$ ; and  $K_h$  (lower unit) =  $4.2 \times 10^{-5}$  and  $8.5 \times 10^{-6} \text{ m s}^{-1}$ .

parameter optimization and evaluation of the results allow for redundancies and checks to assess model performance.

The extreme variability in the observed response of the probes (Fig. 6–8) illustrates the challenges in resolving spatially distributed data sets with a deterministic physics-based model. It is difficult to predict point values of water content through time due to soil heterogeneity (e.g., Wierenga et al., 1991) and processes such as saturation overshoot that cannot be simulated by Richards' equation. Indeed, results indicate that the model cannot adequately reproduce point measurements of water content or matric pressure for all locations at all times. It should also be noted that for all three experiments, the repacked material around the probes was structurally different from the natural soil, especially in the more pedogenically developed Pleistocene soil. Despite these complications, however, the general timing as well as horizontal and vertical extent of the wetting front in response to infiltration and redistribution expressed in the probe data was simulated reasonably well for both the active wash and Holocene soil.

Because the forward model simulations were done assuming diffuse flow, the overall results suggest that this sort of flow, amenable to Richards' equation representation, might dominate most of the water movement at the active wash and Holocene locations, even though the field observations show some features indicative of other flow modes (e.g., saturation overshoot and preferential flow). The model results are limited by the simplifying assumptions of axial symmetry and homogeneity within the

two hydrogeologic units; this model cannot simulate the effects of lateral heterogeneity evidenced by the asymmetry of measured electrical resistivity distributions. In media with relatively little horizontal heterogeneity, such as the active wash deposits considered here, this may not be a serious problem. In some media, however, such as the Pleistocene soil of this study, this sort of heterogeneity is present and probably has substantial ecohydrologic importance (Nimmo et al., 2009). In principle, this inverse approach could be extended to represent greater heterogeneity of the porous media. For example, the modeled domain could be apportioned into additional horizontal as well as vertical zones, each with a set of parameters; however, given the high level of numerical complexity in inverse modeling with a process model that is extremely nonlinear like Richards' equation, such an approach is likely to encounter practical impediments to success.

Geophysical methods are useful for monitoring the overall hydrologic response in the unsaturated zone, as well as characterizing subsurface heterogeneity in soil water and clay content. In particular, these methods provide important information about lateral subsurface flow without considerable disruption of the natural soil structure. The installation of the electrodes at the land surface required only minor disturbance and left the subsurface structure below the infiltration pond undamaged. Conversely, the probes required excavation of six installation holes for each location (all of which were outside the region of the ponded infiltration), which disrupted the zone of interest yet sampled a

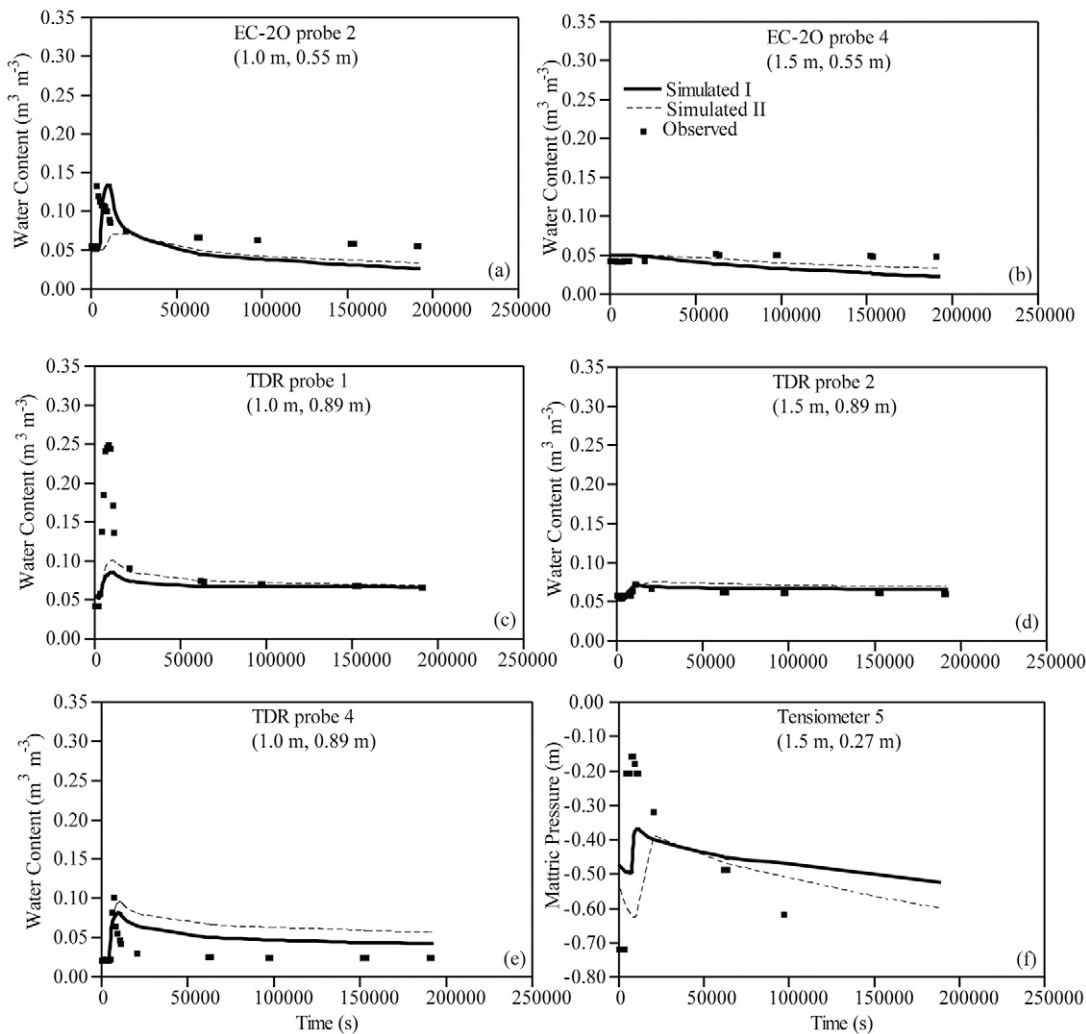


FIG. 7. Time series of observations from selected EC-20 and TDR dielectric constant probes for water content and tensiometers vs. two simulated responses for the Holocene soil. Coordinates of probe placements (radial distance from center of infiltration pond, depth from surface to middle of probe) are given for: (a) EC-20 Probe 2; (b) EC-20 Probe 4; (c) TDR Probe 1; (d) TDR Probe 2 (best fit); (e) TDR Probe 4; and (f) Tensiometer 5 (worst fit). Parameter values used for Simulations I and II, respectively, are: horizontal saturated hydraulic conductivity  $K_h$  (upper unit) =  $2.7 \times 10^{-4}$  and  $1.9 \times 10^{-4} \text{ m s}^{-1}$ ; Rosi-Nimmo water retention curve shape parameters  $\psi_o = 0.31$  and  $0.15 - \text{m}$  and  $\lambda = 6.18$  and  $2.34$ ; and  $K_h$  (lower unit) =  $2.5 \times 10^{-1}$  and  $3.0 \times 10^{-2} \text{ m s}^{-1}$ .

much smaller volume than the ERI. Better techniques are needed for calibrating electrical resistivity data to provide quantitative maps of soil water content (e.g., Singha et al., 2007). Additionally, geophysical methods sensitive to water content must be used in concert with measurements of soil matric pressure to inform a model of soil water movement based on Richards' equation.

Richards' equation lends itself to distributed numerical modeling of subsurface flow, which has the capability to simulate spatially variable values of soil water content through time. Richards' equation utilizes physical parameters that can be constrained using field or laboratory experiments. These advantages are relevant to the intended ecohydrologic applications of this study. One major challenge in applying Richards' equation remains the characterization of subsurface heterogeneity at scales relevant to ecohydrologic applications; geophysical measurements and the inverse method presented here provide a promising approach for this.

## Conclusions

The success of this inverse modeling exercise was considered in the context of the major constraints on the conceptual model imposed by the long-term goal of applying the effective soil hydraulic properties estimated here to a landscape-scale model of the Mojave Desert. The most substantial simplification to the conceptual model for each of the three depositional settings was

that the inherently heterogeneous soils were approximated as two homogeneous, anisotropic hydrogeologic units. Even though the data could theoretically support a more complex conceptual model, the scale of such increased heterogeneity would be smaller than the discretization of the anticipated landscape-scale model. Problems related to the lack of a unique optimal parameter set and poor model performance are not interpreted as failure of the inverse exercise reported here, but rather as an indicator that the conceptual model chosen is not ideal for predicting point measurements in highly heterogeneous, layered systems. Although complex and computationally expensive, the inverse methodology provides a physically more realistic representation of the system than methods that must assume reduced heterogeneity or dimensionality. There is general agreement between representative simulation results and the smoothed wetting front propagation and redistribution of the ERI response for the active wash, as well as good agreement between simulation results and observed probe responses for the active wash and Holocene soil. For the well-developed Pleistocene soil, however, the unexpressed heterogeneity and structure seem to play a more important role in the observed response, such that the simplified conceptual model cannot perform as well at predicting point values or the shape and timing of the subsurface spreading.

There is no single parameter set for any of the three process model scenarios that best represents the corresponding field

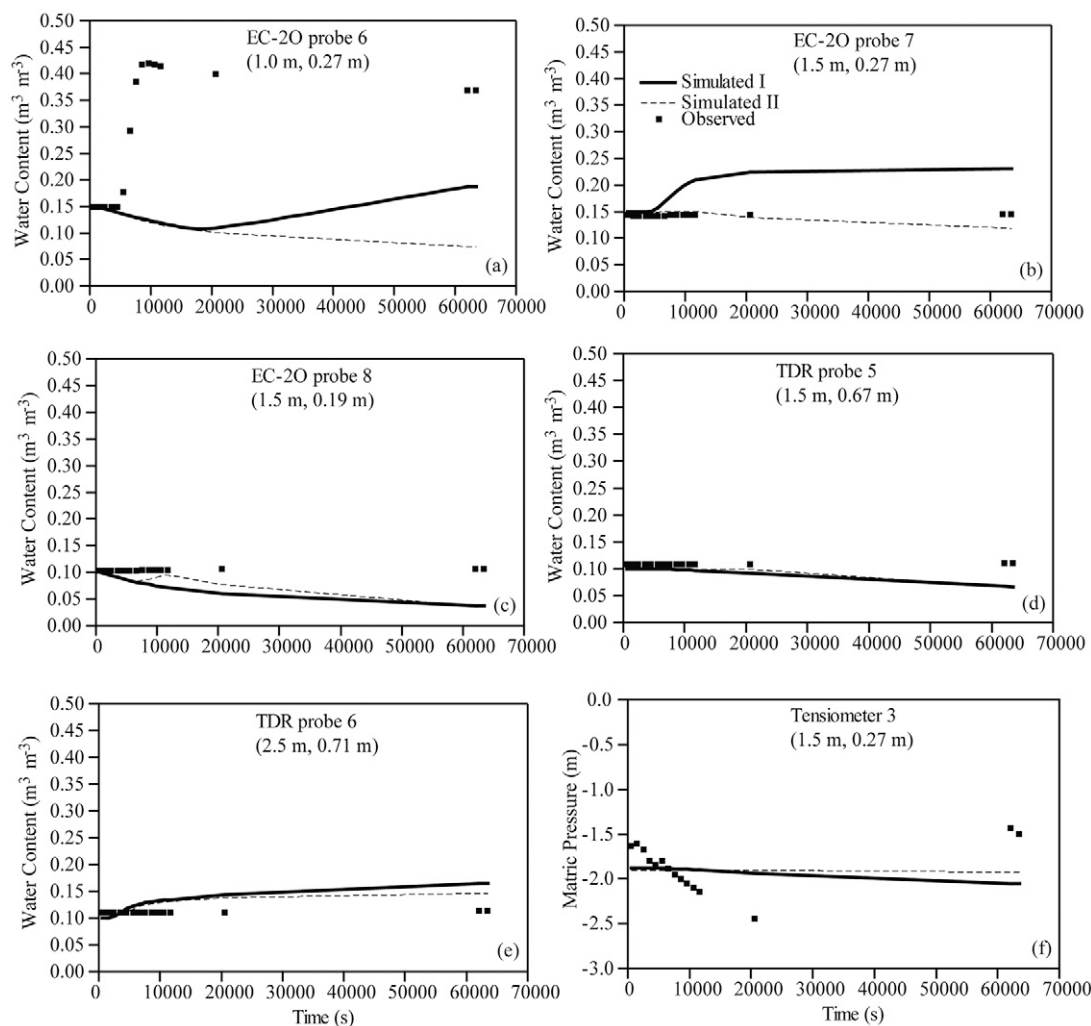


FIG. 8. Time series of observations from selected EC-2O and TDR dielectric constant probes for water content and tensiometers vs. two simulated responses for the Pleistocene soil. Coordinates of probe placements (radial distance from center of infiltration pond, depth from surface to middle of probe) are given for: (a) EC-2O Probe 6 (worst fit); (b) EC-2O Probe 7; (c) EC-2O Probe 8; (d) TDR Probe 5 (best fit); (e) TDR Probe 6; and (f) Tensiometer 3. Parameter values used for Simulations I and II are: horizontal saturated hydraulic conductivity  $K_{h1}$  (upper unit) =  $4.6 \times 10^{-4}$  and  $1.8 \times 10^{-4} \text{ m s}^{-1}$ ; Rossi-Nimmo water retention curve shape parameters  $\psi_o$  (upper unit) = 0.24 and 0.27 -m and  $\lambda$  (upper unit) = 0.21 and 0.31;  $K_{h2}$  (lower unit) =  $4.9 \times 10^{-7}$  and  $6.6 \times 10^{-4} \text{ m s}^{-1}$ ;  $\psi_o$  (lower unit) = 1.73 and 1.60 -m; and  $\lambda$  (lower unit) = 9.23 and 11.30.

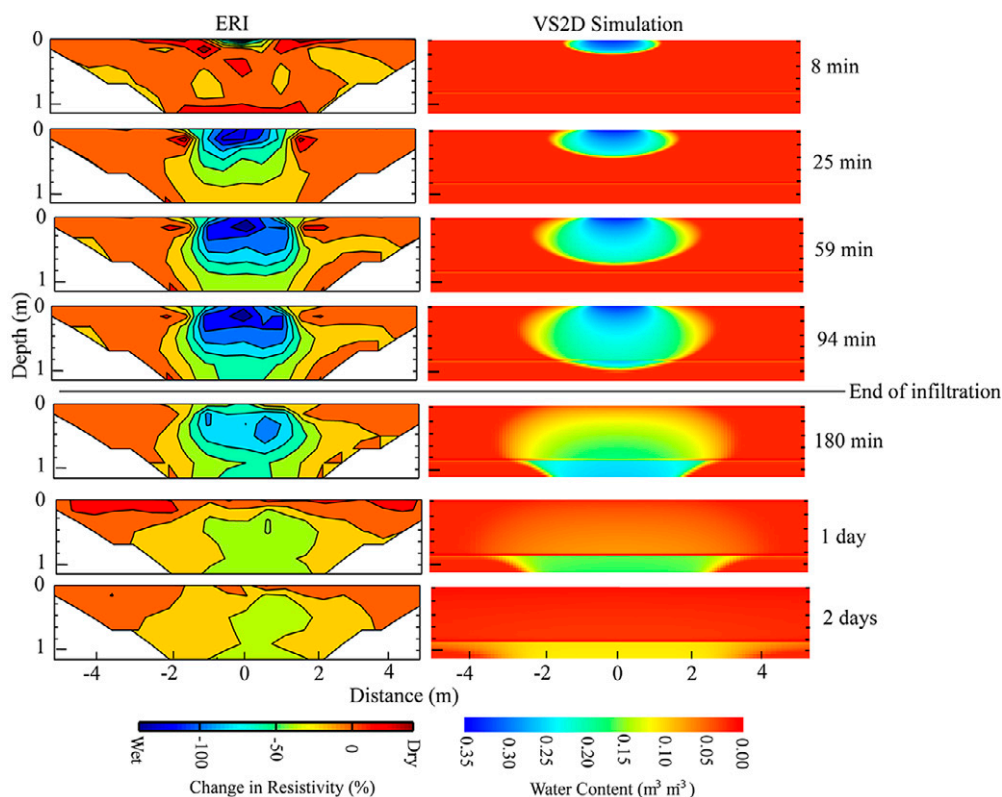


FIG. 9. Snapshot comparisons of the change in electrical resistivity measured by electrical resistivity imaging (ERI) with corresponding VS2D-simulated water contents for the active wash.

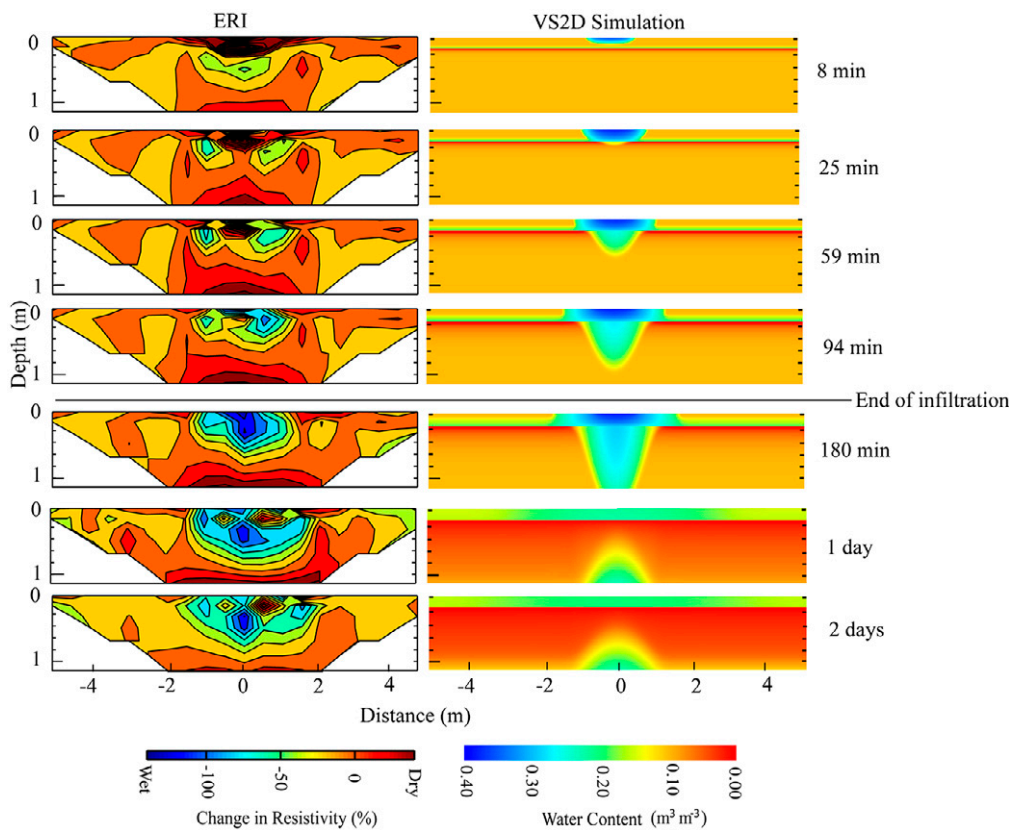


FIG. 10. Snapshot comparisons of the change in electrical resistivity measured by electrical resistivity imaging (ERI) with corresponding VS2D-simulated water contents for the Pleistocene soil.

observations. The detail expressed in the process model scenarios is consistent with the level of complexity to be implemented in the landscape-scale model of soil moisture dynamics. For the long-term goals of this effort—the expression of lateral and vertical soil moisture distribution as it relates to landscape-scale planning initiatives—the results demonstrate a reasonable framework for assigning effective parameter values based on soil age and type.

Our results illuminate the relative utility of effective soil hydraulic properties for quantifying the combined horizontal and vertical fluxes of soil moisture for a regional-scale model of soil moisture dynamics. Although the conceptual model performed reasonably well, quantifying the horizontal fluxes of soil moisture relevant to desert ecosystems (Nimmo et al., 2009) would require greater degrees of heterogeneity than presently included. A more complex conceptual model and subsequent inverse problem may require global optimization techniques (e.g., Vrugt et al., 2004; Schoups et al., 2005), which have been used for estimating spatially variable soil hydraulic properties of complex distributed systems. Future work will need to further investigate hydraulic properties and the role of heterogeneity in older desert soils with well-developed Av horizons before proceeding to a landscape-scale model of soil moisture dynamics.

#### ACKNOWLEDGMENTS

We are grateful for funding from the Mojave Desert Department of the Interior (DOI) on the Landscape program. Thanks to Rick Healy for promptly providing the Rossi–Nimmo modifications to VS2D. Thanks to Claire Tiedeman for advice and support with UCODE and her thoughtful comments. We greatly appreciate the insightful comments and suggestions from Brian Andraski and Brian Ebel on an earlier version of this manuscript.

## References

- al Hagrey, S.A., and J. Michaelsen. 1999. Resistivity and percolation study of preferential flow in vadose zone at Bokhorst, Germany. *Geophysics* 64:746–753.
- Baveye, P., H. Rogasik, O. Wendroth, I. Onasch, and J.W. Crawford. 2002. Effect of sampling volume on the measurement of soil physical properties: Simulation with x-ray tomography data. *Meas. Sci. Technol.* 13:775–784.
- Binley, A., and K. Beven. 2003. Vadose zone flow model uncertainty as conditioned on geophysical data. *Ground Water* 41:119–127.
- Binley, A., P. Winship, R. Middleton, M. Poker, and J. West. 2001. High resolution characterization of vadose zone dynamics using cross-borehole radar. *Water Resour. Res.* 37:2639–2652.
- Bitterlich, S., W. Durner, S.C. Iden, and P. Knabner. 2004. Inverse estimation of the unsaturated soil hydraulic properties from column outflow experiments using free-form parameterizations. *Vadose Zone J.* 3:971–981.
- Constantz, J., and W.N. Herkelrath. 1984. An improved pressure outflow cell for measurement of pore water properties from 0 to 10°C. *Soil Sci. Soc. Am. J.* 48:7–10.
- DiCarlo, D.A. 2004. Experimental measurements of saturation overshoot on infiltration. *Water Resour. Res.* 40:W04215, doi:10.1029/2003WR002670.
- Glass, R.J., J.R. Brainard, and J. Yeh. 2005. Infiltration in unsaturated layered fluvial deposits at Rio Bravo: Macroscopic anisotropy and heterogeneous transport. *Vadose Zone J.* 4:22–31.
- Hill, M.C., and C.R. Tiedeman. 2007. *Effective groundwater model calibration: With analysis of data, sensitivities, predictions, and uncertainty.* John Wiley & Sons, New York.
- Hsieh, P.A., W. Wingle, and R.W. Healy. 2000. VS2DI: A graphical software package for simulating fluid flow and solute or energy transport in variably saturated porous media. *Water-Resour. Invest. Rep.* 99–4130. USGS, Reston, VA.
- Hopmans, J.W., D.R. Nielsen, and K.L. Bristow. 2002a. How useful are small-scale soil hydraulic property measurements for large-scale vadose zone modeling? p. 247–258. *In* D. Smiles et al. (ed.) *Environmental mechanics: Water, mass and energy transfer in the biosphere.* Geophys. Monogr. 129. Am. Geophys. Union, Washington, DC.

- Hopmans, J.W., and J. Šimůnek. 1999. Review of inverse estimation of soil hydraulic properties. p. 643–659. *In* M.Th. van Genuchten et al. (ed.) Characterizations and measurement of the hydraulic properties of unsaturated porous media. Proc. Int. Worksh., Riverside, CA. 22–24 Oct. 1997. U.S. Salinity Lab., Riverside, CA.
- Hopmans, J.W., J. Šimůnek, N. Romano, and W. Durner. 2002b. Simultaneous determination of water transmission and retention properties: Inverse methods. p. 963–1008. *In* J.H. Dane and G.C. Topp (ed.) Methods of soil analysis. Part 4. Physical methods. SSSA Book Ser. 5. SSSA, Madison, WI.
- Kohne, J.M., B.P. Mohanty, and J. Šimůnek. 2005. Inverse dual-permeability modeling of preferential water flow in a soil column and implications for field-scale solute transport. *Vadose Zone J.* 5:59–76.
- Lambot, S., F. Hupet, M. Javaux, and M. Vanclooster. 2004. Laboratory evaluation of a hydrodynamic inverse modeling method based on water content data. *Water Resour. Res.* 40:W03506, doi:10.1029/2003WR002641.
- Lappala, E.G., R.W. Healy, and E.P. Weeks. 1987. Documentation of computer program VS2D to solve the equations of fluid flow in variably saturated porous media. *Water-Resour. Invest. Rep.* 83-4099. USGS, Reston, VA.
- Mertens, J., R. Stenger, and G.F. Barkle. 2006. Multiobjective inverse modeling for soil parameter estimation and model verification. *Vadose Zone J.* 5:917–933.
- Miller, D.M., D.R. Bedford, D.L. Hughson, E.V. McDonald, S.E. Robinson, and K.M. Schmidt. 2009. Mapping Mojave Desert ecosystem properties with surficial geology. p. 225–251. *In* R.H. Webb et al. (ed.) The Mojave Desert, ecosystem processes and sustainability. University of Nevada Press, Reno.
- Mualem, Y. 1976. A new model for predicting the hydraulic conductivity of unsaturated porous media. *Water Resour. Res.* 12:513–522.
- Mualem, Y. 1984. Anisotropy of unsaturated soils. *Soil Sci. Soc. Am. J.* 48:505–509.
- National Research Council. 2001. Conceptual models of flow and transport in the fractured vadose zone. Natl. Acad. Press, Washington, DC.
- Nimmo, J.R., and K.S. Perkins. 2008. Effect of soil disturbance on recharging fluxes: Case study on the Snake River Plain, Idaho National Laboratory, USA. *Hydrogeol. J.* 16:829–844.
- Nimmo, J.R., K.S. Perkins, K.M. Schmidt, J.D. Stock, D.M. Miller, and K. Singha. 2009. Hydrologic characterization of desert soils with varying degrees of pedogenesis: 1. Field experiments evaluating plant-relevant soil water behavior. *Vadose Zone J.* 8:480–496 (this issue).
- Nimmo, J.R., K.M. Schmidt, K.S. Perkins, and J.D. Stock. 2008. Method for rapid measurement of field-saturated hydraulic conductivity over rugged landscapes. *Vadose Zone J.* 8:142–149.
- Pachepsky, Y.A., A.K. Guber, M.Th. van Genuchten, T.J. Nicholson, R.E. Cady, J. Šimůnek, and M.G. Schaap. 2006. Model abstraction techniques for soil water flow and transport. NUREG CR-6884. U.S. Nuclear Regulatory Commission, Washington, DC.
- Poeter, E.P., M.C. Hill, E.R. Banta, S. Mehl, and S. Christensen. 2005. UCODE\_2005 and six other computer codes for universal sensitivity analysis, calibration, and uncertainty evaluation. *Tech. Methods* 6-A11. USGS, Reston, VA.
- Reynolds, W.D., and D.E. Elrick. 1990. Ponded infiltration from a single ring: I. Analysis of steady flow. *Soil Sci. Soc. Am. J.* 54:1233–1241.
- Robinson, D.A., A. Binley, N. Crook, F.D. Day-Lewis, T.P.A. Ferré, V.J.S. Grauch, et al. 2008. Advancing process-based watershed hydrological research using near-surface geophysics: A vision for, and review of, electrical and magnetic geophysical methods. *Hydrol. Processes* 22:3604–3635.
- Robinson, D.A., S.B. Jones, J.M. Wraith, D. Or, and S.P. Friedman. 2003. A review of advances in dielectric and electrical conductivity measurement in soils using time domain reflectometry. *Vadose Zone J.* 2:444–475.
- Rose, C.W., W.R. Stern, and J.E. Drummond. 1965. Determination of hydraulic conductivity as a function of depth and water content for soil *in situ*. *Aust. J. Soil Res.* 3:1–9.
- Ross, P.J., J. William, and K.L. Bristow. 1991. Equation for extending water-retention curves to dryness. *Soil Sci. Soc. Am. J.* 55:923–927.
- Rossi, C., and J.R. Nimmo. 1994. Modeling of soil water retention from saturation to oven dryness. *Water Resour. Res.* 30:701–708.
- Schoups, G.H., J.W. Hopmans, C.A. Young, J.A. Vrugt, and W.W. Wallender. 2005. Multi-criteria optimization of a regional spatially-distributed subsurface water flow model. *J. Hydrol.* 311:20–48.
- Schwartz, R.C., and S.R. Evett. 2003. Conjective use of tension infiltrometry and time-domain reflectometry for inverse estimation of soil hydraulic properties. *Vadose Zone J.* 2:530–538.
- Schwartzel, K., J. Šimůnek, H. Stroffregen, G. Wessolek, and M. Th. van Genuchten. 2006. Estimation of the unsaturated hydraulic conductivity of peat soils: Laboratory versus field data. *Vadose Zone J.* 5:628–640.
- Singha, K., F.D. Day-Lewis, and S. Moysey. 2007. Accounting for tomographic resolution in estimating hydrologic properties from geophysical data. p. 227–242. *In* D.W. Hyndman et al. (ed.) Subsurface hydrology: Data integration for properties and processes. *Geophys. Monogr.* 171. Am. Geophys. Union, Washington, DC.
- Stephens, D.B., and S. Heermann. 1988. Dependence of anisotropy on saturation in a stratified sand. *Water Resour. Res.* 24:770–778.
- Stonestrom, D.A., and K.C. Akstin. 1994. Nonmonotonic matric pressure histories during constant flux infiltration into homogeneous profiles. *Water Resour. Res.* 30:81–91.
- Vachaud, G., and J.H. Dane. 2002. Instantaneous profile. p. 937–945. *In* J.H. Dane and G.C. Topp (ed.) Methods of Soil Analysis. Part 4. Physical methods. SSSA Book Ser. 5. SSSA, Madison, WI.
- Vereecken, H., R. Kasteel, J. Vanderborght, and T. Harter. 2007. Upscaling hydraulic properties and soil water flow processes in heterogeneous soils: A review. *Vadose Zone J.* 6:1–28.
- Vrugt, J.A., W. Bouten, H.V. Gupta, and S. Sorooshian. 2002. Toward improved identifiability of hydrologic model parameters: The information content of experimental data. *Water Resour. Res.* 38(12):1312, doi:10.1029/2001WR001118.
- Vrugt, J.A., G. Schoups, J.W. Hopmans, C. Young, W.W. Wallender, T. Harter, and W. Bouten. 2004. Inverse modeling of large-scale spatially distributed vadose zone properties using global optimization. *Water Resour. Res.* 40:W06503, doi:10.1029/2003WR002706.
- Vrugt, J.A., P.H. Stauffer, Th. Wöhling, B.A. Robinson, and V.V. Vesselinov. 2008. Inverse modeling of subsurface flow and transport properties: A review with new developments. *Vadose Zone J.* 7:843–864.
- Ward, A.L., and Z.F. Zhang. 2007. Effective hydraulic properties determined from transient unsaturated flow in anisotropic soils. *Vadose Zone J.* 6:913–924.
- Wierenga, P.J., R.G. Hills, and D.B. Hudson. 1991. The Las Cruces trench site: Characterization, experimental results, and one-dimensional flow predictions. *Water Resour. Res.* 27:2695–2705.
- Winfield, K.A., J.R. Nimmo, J.A. Izbicki, and P.M. Martin. 2006. Resolving structural influence on water-retention properties of alluvial deposits. *Vadose Zone J.* 5:706–719.
- Yeh, T.J., M. Ye, and R. Khaleel. 2005. Estimation of effective unsaturated hydraulic conductivity tensor using spatial moments of observed moisture plume. *Water Resour. Res.* 41:W03014, doi:10.1029/2004WR003736.
- Zhang, Z.F., A.L. Ward, and G.W. Gee. 2003. Estimating soil hydraulic parameters of a field drainage experiment using inverse techniques. *Vadose Zone J.* 2:201–211.
- Zhou, Q.Y., J. Shimada, and A. Sato. 2001. Three-dimensional spatial and temporal monitoring of soil water content using electrical resistivity tomography. *Water Resour. Res.* 37:273–285.